

Parity violation in charged-particle resonance reactions

G. E. Mitchell¹ and J. F. Shriner, Jr.²

¹North Carolina State University, Raleigh, North Carolina 27695
and Triangle Universities Nuclear Laboratory, Durham, North Carolina 27708

²Tennessee Technological University, Cookeville, Tennessee 38505

(Received 12 February 1996)

Parity nonconservation (PNC) measurements utilizing charged-particle resonance reactions are proposed. PNC observables have been calculated for over 300 resonance pairs (with the same angular momentum and opposite parity) in five *s-d* shell nuclei. Detailed numerical results are presented for the longitudinal analyzing powers in the $^{31}\text{P}(\vec{p}, \alpha_0)$ reaction. There is strong dependence on energy, angle, and resonance parameters. A figure of merit that includes both the relative enhancement of the parity violation and the cross section is used to identify the most promising resonances for study. A proposed detector design and experimental procedure are described. These measurements should provide information on the weak spreading width (the effective nucleon-nucleus weak interaction) in light nuclei. [S0556-2813(96)00907-7]

PACS number(s): 24.80.+y, 24.60.Dr, 25.40.Ny, 11.30.Er

I. INTRODUCTION

A. Background

The traditional view towards symmetry breaking in the nucleus is exemplified by the approach to parity violation in light nuclei. Parity doublets (closely spaced, low-lying states of the same angular momentum and opposite parity) were studied. The major difficulty is the determination of the nuclear wave function with sufficient accuracy. Even after the discovery [1] of a very large enhancement of parity violation for neutron resonances in heavy nuclei (as large as 10^6), these new measurements were considered of only anecdotal interest, since one did not (indeed could not) know the wave functions for these complicated systems. A new approach adopts the view that a highly excited nuclear system is chaotic, and treats the symmetry-breaking matrix elements as random variables. The goal of the experiment is to determine the root-mean-square symmetry-breaking matrix element. This change of emphasis means that several measurements (rather than only one) are required to extract relevant information. The compound nucleus is now considered as an excellent laboratory for the study of symmetry breaking [2,3]. For a measure of the profound change in attitude, compare the classic review by Adelberger and Haxton [4] with the recent review by Bowman *et al.* [3].

A comprehensive review of the early measurements with polarized neutrons is given by Krupchitsky [5]. In all of these measurements the parity violations are large compared to the nucleon-nucleon scale of 10^{-7} , but still are small compared to one. Sushkov and Flambaum [6,7] suggested that the mechanism of compound-nuclear mixing between closely opposite parity states with the same total angular momentum *J* could lead to large parity violations. Alfimenkov *et al.* [1] measured the helicity dependence of the neutron total cross section and observed an extremely large parity violation ($\approx 7\%$) at the 0.73-eV resonance in ^{139}La . This effect later was confirmed at IAE [8], KEK [9], and Los Alamos [10]. Parity nonconservation (PNC) had also been observed in several other nuclei (see, e.g., [1,11–14]). In all of these experiments, however, only one parity violation was

measured per nuclide. This is a crucial limitation, since a number of measurements are required for the statistical analysis.

The TRIPLE collaboration has measured a number of parity violations in a given nuclide [15–17] (providing data suitable for the determination of a rms PNC matrix element) and for a variety of nuclides (providing data to examine the mass dependence of the weak nucleon-nucleus interaction). The neutron measurements have been performed only for targets which are near the maxima of the $3p$ and $4p$ neutron strength function. The available data (near $A=110$ and $A=230$) do not provide a broad dynamic range in *A* and have rather large uncertainties, thus making measurements in lighter nuclei of particular value.

Unfortunately, the larger level spacing for light nuclei means that a completely different experimental system is required to perform the neutron transmission experiments. In this context we initiated a study of alternative parity-violation experiments that maintained the statistical approach [18]. It is natural to introduce a spreading width in order to compare results from nuclei with different level densities. In the following we focus on determining the weak spreading width in the $2s-1d$ shell.

B. Charged-particle experiments

Charged-particle resonance experiments might appear much less promising for the study of parity violation than are neutron resonances, but the relative merit of the proton and neutron experiments depends on the mass number *A*. For lighter nuclei (e.g., *A* near 30) the large level spacing means that in order to study a number of resonances, the bombarding energy must be MeV, not eV. This increase in energy means that the neutron experiment is much more difficult than the corresponding charged-particle experiment, while the major advantage of strong kinematic enhancement is lost. For charged particles, the possibility of easily studying several reaction channels and the greater ease of measuring differential cross sections makes determination of the nuclear spectroscopic information much simpler. This latter informa-

tion, which is essential for extracting a PNC matrix element, is available from earlier measurements in our laboratory for five target nuclides in the nuclear $2s-1d$ shell [19–25].

Of course, to justify the use of the statistical approach to the analysis, it is essential that the compound-nuclear states behave statistically. Our conclusion that a statistical description of these resonance states is suitable is based on the spacing distributions for a range of nuclei in this mass region [26,27], on spacing distributions of shell model states [28], and on characteristics of the distributions of shell model eigenfunctions [29].

In Sec. II we outline a description of parity violation in nuclear reactions (in the two-level approximation), and obtain the longitudinal asymmetry. Although we have calculated the parity violation for both elastic scattering and the (p, α) reaction, and for both transverse polarizations (analyzing power A_x) and longitudinal polarizations (analyzing power A_z), here we focus on A_z for the (p, α) reaction (the analyzing powers are larger for the reaction and measuring A_z is easier than measuring A_x). We calculated the analyzing powers for targets with spin $I=1/2, 3/2,$ and $5/2$ and for resonances with total angular momentum $J=1, 2, 3,$ and 4 . We considered parity doublets for the (p, α) reaction on $^{23}\text{Na}, ^{27}\text{Al}, ^{31}\text{P}, ^{35}\text{Cl},$ and ^{39}K . To conserve space we shall not present the very lengthy expressions for the longitudinal asymmetries; nor shall we present results in detail for all target nuclides. We focus on ^{31}P , which appears to be the best candidate target for a PNC measurement with charged-particle resonances. In Sec. III we list the relevant resonances and their relative enhancements for the compound nucleus ^{32}S . In Sec. IV the enhancements and the figures of merit (which incorporate both the enhancement and the cross section) are shown graphically for several resonance pairs. Angular and multilevel effects also are considered. In Sec. V a proposed PNC experiment is outlined and numerical examples presented. The final section is a brief summary.

II. THEORY

In this section we present the expressions needed to evaluate the longitudinal analyzing power A_z for a pair of interfering resonances with the same J but different parity. The results will be expressed in terms of the energies E_n and E_u of the natural- and unnatural-parity resonances, respectively, the total widths Γ_n and Γ_u , and the partial widths Γ_{nc} and Γ_{uc} . Partial reduced width amplitudes will be denoted γ_{nc} and γ_{uc} ; a partial width and the corresponding reduced width are related in the usual way:

$$\Gamma_c = 2P_c \gamma_c^2, \quad (1)$$

where P_c is the penetrability in channel c .

We considered the (p, α_0) reaction on the five $A=4n-1$ nuclides $^{23}\text{Na}, ^{27}\text{Al}, ^{31}\text{P}, ^{35}\text{Cl},$ and ^{39}K ; in each case, the ground state of the residual nucleus has angular momentum and parity 0^+ . Thus, there is only a single parity-allowed exit channel, corresponding to alpha emission from the natural-parity compound state with orbital angular momentum $\ell=J$ and channel spin $s'=0$. Since the target nuclides do not have spin zero, the entrance channel for either state will in general show ℓ mixing and/or channel spin

mixing [30]. Therefore, there is more than one parity-allowed entrance channel for each resonance. We use p and q , respectively, to denote the parity-allowed proton channels for the natural- and unnatural-parity levels. The partial channels to be considered for a (p, α_0) reaction are $\aleph=p+q+1$ in number, with channels $1, 2, \dots, p$ the entrance channels that are parity allowed for the natural-parity resonance, channels $p+1, p+2, \dots, p+q$ the entrance channels that are parity allowed for the unnatural-parity resonance, and channel \aleph the parity-allowed alpha particle channel.

We assume a Hamiltonian of the form

$$H = H_{\text{PC}} + H_{\text{PNC}}, \quad (2)$$

which contains both a parity-conserving term and a (small) parity-violating term; the matrix element of H_{PNC} between the natural-parity state and the unnatural-parity state is denoted by V . We assume that any parity violation occurs in the compound states (internal mixing) and not in the entrance or exit channels (external mixing). Since V is small, all terms higher than first order in V will be ignored.

It is convenient to use the R -matrix formalism [31] to derive the elements of the collision matrix S . We use first-order perturbation theory to generate the reduced width amplitudes. If we denote an unperturbed amplitude by γ^0 , then

$$\begin{aligned} \gamma_{nc}^0 &= 0, & c &= p+1, \dots, p+q, \\ \gamma_{uc}^0 &= 0, & c &= 1, \dots, p, \\ \gamma_{uc}^0 &= 0, & c &= \aleph. \end{aligned} \quad (3)$$

The perturbed amplitudes can then be expressed as

$$\begin{aligned} \gamma_{nc} &= \gamma_{nc}^0, & c &= 1, \dots, p, \\ \gamma_{nc} &= \frac{V}{E_n - E_u} \gamma_{uc}^0, & c &= p+1, \dots, p+q, \\ \gamma_{nc} &= \gamma_{nc}^0, & c &= \aleph, \\ \gamma_{uc} &= \frac{V}{E_u - E_n} \gamma_{nc}^0, & c &= 1, \dots, p, \\ \gamma_{uc} &= \gamma_{uc}^0, & c &= p+1, \dots, p+q, \\ \gamma_{uc} &= \frac{V}{E_u - E_n} \gamma_{nc}^0, & c &= \aleph. \end{aligned} \quad (4)$$

For this two-level, \aleph -channel problem, the level matrix provides the most suitable approach. The elements of the level matrix can be written

$$\begin{aligned} A_{nn} &= \frac{E_u - E - i\Gamma_u/2}{\Delta}, \\ A_{uu} &= \frac{E_n - E - i\Gamma_n/2}{\Delta}, \\ A_{nu} &= A_{un} = -\frac{iV}{2\Delta} \frac{\Gamma_n - \Gamma_u}{E_n - E_u}, \end{aligned} \quad (5)$$

where

$$\Delta = (E_n - E - i\Gamma_n/2)(E_u - E - i\Gamma_u/2). \quad (6)$$

The collision matrix S is given in matrix form by

$$S = \Omega^2 + 2i\Omega P^{1/2} U P^{1/2} \Omega, \quad (7)$$

where Ω is a phase matrix, P is the penetrability matrix, and U is defined in terms of the level matrix and reduced width amplitudes,

$$U_{cc'} = \sum_{\lambda\rho} (\gamma_\lambda \times \gamma_\rho)_{cc'} A_{\lambda\rho}. \quad (8)$$

For the (p, α_0) reaction with only internal mixing, the only first-order parity-violating terms of S correspond to entrance in one of the proton channels of the unnatural-parity resonance and exit via the alpha channel. Parity-conserving terms of S will correspond to entrance through one of the proton channels of the natural-parity resonance and exit through the alpha channel. The S -matrix elements for these cases can be written

$$S_{c\aleph} = \frac{ie^{i(\xi_c + \xi_\aleph)} g_c g_\aleph}{E_n - E - i\Gamma_n/2}, \quad c = 1, \dots, p,$$

$$S_{c\aleph} = \frac{-ie^{i(\xi_c + \xi_\aleph)} g_c g_\aleph V}{(E_n - E - i\Gamma_n/2)(E_u - E - i\Gamma_u/2)},$$

$$c = p + 1, \dots, p + q. \quad (9)$$

The longitudinal analyzing power is defined by

$$A_z \equiv \frac{(d\sigma/d\Omega)(\rightarrow) - (d\sigma/d\Omega)(\leftarrow)}{(d\sigma/d\Omega)(\rightarrow) + (d\sigma/d\Omega)(\leftarrow)}, \quad (10)$$

where \rightarrow (\leftarrow) denotes beam polarization parallel (antiparallel) to the beam direction. The differential cross section for reactions with polarized beam has been discussed by several authors (see, e.g., [32–34]) and can be written in this case as

$$\frac{d\sigma}{d\Omega} = 4\pi^2 \chi^2 \sum \frac{(-1)^{I+k_i+\ell_2-i-s_2+\ell_2'+s'+k-\ell_1'-J}}{(4\pi)^{3/2}} \frac{\hat{k}_i \hat{k}_\ell \hat{\ell}_1 \hat{\ell}_2 \hat{s}_1 \hat{s}_2 \hat{J}^2}{\hat{k} \hat{I}^2} (k_i n k_\ell 0 | k n) (\ell_1 0 \ell_2 0 | k_\ell 0) W(is_1 is_2 | Ik_i) \times \begin{bmatrix} s_1 & \ell_1 & J \\ s_2 & \ell_2 & J \\ k_i & k_\ell & k \end{bmatrix} \bar{Z}(\ell_1' J \ell_2' J; s' k) \rho_{k_i n} Y_{kn}(\theta, \phi) \langle s' \ell_1' | S | s_1 \ell_1 \rangle \langle s' \ell_2' | S | s_2 \ell_2 \rangle^*. \quad (11)$$

Here the quantities in parentheses are Clebsch-Gordan coefficients [35], \bar{Z} is the Z coefficient of Biedenharn, Blatt, and Rose [36] as modified by Huby [37], and the quantity in brackets is a $9j$ coefficient [35]. The quantities ℓ (ℓ') and s (s') are the orbital angular momentum and channel spin in the entrance (exit) channel, i and I are the spins of the projectile and target, respectively, J is the spin of the compound states, Y_{kn} is a spherical harmonic, and $\rho_{k_i n}$ is the density tensor describing the beam polarization. The notation \hat{I} denotes the quantity $\sqrt{2I+1}$. The summation is over all possible values allowed by the angular momentum coupling coefficients given a particular choice of J and I . When Eqs. (9) and (11) are inserted into Eq. (10), the numerator of A_z is (to first order) proportional to V ; the denominator of A_z is twice the unpolarized cross section and is independent of V . Because of the complexity of A_z for given values of J and I , we do not include any explicit expressions. Calculations of A_z actually proceeded in two steps: The denominator is evaluated using a multilevel, multichannel R -matrix code [30], while the numerator is determined by evaluating only the terms in A_z that depend on V .

III. RESONANCE PARAMETERS AND ENHANCEMENTS

As noted in the Introduction, our group obtained detailed spectroscopic results for resonances in five s - d shell nuclei.

Here we focus on the results for protons on ^{31}P [22]. In Table I the resonance energies, total widths, and J values are listed for pairs of resonances in $p + ^{31}\text{P}$ reactions. Pairs are listed for resonances with the same J value and opposite parity which are separated by an energy difference less than 10 times the sum of the total widths of the two resonances.

Since A_z is proportional to V , it is convenient to use the value of A_z/V as a measure of the relative enhancement of PNC effects. However, a large relative enhancement can occur either because of a large difference in cross section for the two helicities (a large numerator), or because of a small cross section (a small denominator). The appropriate figure of merit which combines the cross section and A_z is

$$\beta_P \equiv \left(\frac{A_z}{V} \right)^2 \frac{d\sigma}{d\Omega}. \quad (12)$$

A large value of β_P indicates a shorter time to reach a specific statistical uncertainty in V .

The experiment measures A_z , not the relative enhancement A_z/V , and therefore the magnitude of A_z is the real quantity of interest. The matrix element V is assumed to be a random variable and is the quantity that we wish to determine. However, one can use an estimate for V_{rms} , and then

TABLE I. Resonance energies, total widths, and J values for pairs of resonances in $p + {}^{31}\text{P}$. Pairs listed are those separated by an energy difference less than 10 times the sum of the two total widths. The subscript n denotes the natural parity resonance of the pair, while the subscript u denotes the unnatural parity resonance.

Resonance pair	E_n (MeV)	E_u (MeV)	Γ_n (keV)	Γ_u (keV)	J
1	1.6433	1.5875	1.7	7.0	0
2	1.9756	1.9669	0.15	5.0	2
3	1.9890	1.9669	0.16	5.0	2
4	1.8938	1.9810	21	0.75	1
5	2.0220	1.9810	22	0.75	1
6	2.2575	2.1808	4.2	6.7	2
7	2.7067	2.7290	0.50	32	2
8	2.8289	2.7920	0.81	32	2
9	2.9064	2.7290	2.6	32	2
10	2.9497	2.7290	2.8	32	2
11	2.8110	2.8484	1.6	5.5	1
12	2.8340	2.8484	19	5.5	1
13	2.8545	2.8484	27	5.5	1
14	2.8340	2.8651	19	0.80	1
15	2.8545	2.8651	27	0.80	1
16	2.8340	2.9776	19	0.90	1
17	2.8545	2.9776	27	0.90	1
18	2.9640	2.9776	24	0.90	1
19	3.0356	3.0341	2.0	0.12	3
20	2.9064	3.0500	2.6	19	2
21	2.9497	3.0500	2.8	19	2
22	3.2376	3.0500	2.0	19	2
23	3.2515	3.0500	9.0	19	2
24	3.2597	3.0500	2.6	19	2
25	2.9640	3.1839	24	2.5	1
26	3.0380	3.1839	37	2.5	1
27	3.1452	3.1839	6.3	2.5	1
28	3.2376	3.1963	2.0	8.6	2
29	3.2515	3.1963	9.0	8.6	2
30	3.2597	3.1963	2.6	8.6	2
31	3.3845	3.3941	3.2	0.33	3
32	3.3963	3.3941	4.3	0.33	3
33	3.0380	3.4260	37	3.5	1
34	3.4280	3.4260	10	3.5	1
35	3.4390	3.4260	5.5	3.5	1
36	3.4280	3.7250	10	26	1
37	3.4390	3.7250	5.5	26	1
38	3.5430	3.7250	15	26	1
39	3.5841	3.7250	2.8	26	1
40	3.6404	3.7250	4.2	26	1
41	3.9006	3.7250	2.8	26	1
42	4.0000	3.7250	30	26	1
43	3.7670	3.8230	4.6	2.9	2
44	3.7945	3.8230	9.1	2.9	2
45	3.8473	3.8230	2.0	2.9	2
46	3.8529	3.8230	0.40	2.9	2

consider the product $(A_z/V)V_{\text{rms}}$ as an estimate for the analyzing power. An estimate for V_{rms} can be obtained from the spreading width

$$\Gamma_p \equiv 2\pi \frac{\langle V^2 \rangle}{D}, \quad (13)$$

where D is the average level spacing. Based on the experimental behavior of the isospin-violating spreading width [38] and on statistical arguments given by [3], we assume that the weak spreading width is constant and equal to the value 3×10^{-7} eV determined in the neutron measurements on heavy nuclei [15,16] near the $4p$ neutron strength function maximum. This is the simplest assumption and is also consistent with the preliminary experimental results [17] near the $3p$ neutron strength function maximum. The average spacing D was determined from the experimental resonance data as a function of both J and E . Therefore one has an estimate for V_{rms} for each resonance pair. In Table II are listed the maximum figure of merit (there is a strong angular and energy dependence of β_p , which we discuss below), the angle at which the figure of merit is largest (calculations were performed in the center-of-mass frame between the angles 90° and 178° in steps of 2°), and the corresponding cross section, relative enhancement, and estimated value of A_z for each resonance pair in $p + {}^{31}\text{P}$. To simulate a realistic experiment, the cross sections were convoluted with a Gaussian resolution function of 500 eV full width at half maximum (FWHM) before A_z was calculated.

The estimates for A_z range from about 1×10^{-6} to 6×10^{-3} , while the corresponding estimates of V_{rms} from Eq. (13) range from about 50 to 150 meV. (Note that in heavy nuclei the values of V_{rms} extracted from the data are about 1 meV, while longitudinal asymmetries as large as 10^{-1} have been measured.) The strong energy and angular effects are discussed in the next section.

IV. EXAMPLES

A. Energy and angular dependence

In Fig. 1 the relative enhancement A_z/V is plotted for four resonance pairs in the ${}^{31}\text{P}(p, \alpha_0)$ reaction. The enhancement is strongly dependent on both energy and angle. This behavior is similar to that observed in a study of detailed-balance tests of time-reversal invariance with interfering resonances [39,40]. Of special importance is the fact that the relative enhancement often changes sign with angle—this sign change in A_z/V , and therefore in A_z , leads to the requirement (discussed below) that the particle detectors must be segmented in angle. The enhancement normally shows a rather narrow single peak as a function of energy, but secondary maxima are frequent. The other 327 pairs studied (42 other pairs for ${}^{31}\text{P}$ and 285 pairs for the other four nuclei) show similar behavior.

Figure 2 shows the angular and energy dependence of the figure of merit β_p for the same four resonance pairs as shown in Fig. 1. Since the figure of merit is intrinsically positive, these results are easier to interpret visually. Again, the most notable feature is the strong dependence on both energy and angle. Results for other resonance pairs for ${}^{31}\text{P}$

TABLE II. Figures of merit and associated parameters for each resonance pair in $^{31}\text{P}(\vec{p}, \alpha_0)$. The calculations assume a resolution of 500 eV FWHM.

Resonance pair	Maximum β_p [10^{-6} mb/(sr eV ²)]	E_p^a (MeV)	θ_{lab}^a (deg)	$d\sigma/d\Omega^a$ (mb/sr)	A_z/V^a ($10^{-4}/\text{eV}$)	Est. A_z^a (10^{-5})
1	0.036	1.6433	90	6.4	0.75	2.0
2	16	1.9756	178	31	-7.2	-7.3
3	4.9	1.9890	124	9.5	7.2	7.3
4	0.020	1.9810	178	2.6	-0.88	-0.89
5	0.12	1.9810	178	2.6	2.2	2.2
6	0.098	2.2574	128	6.8	1.2	1.2
7	3.0	2.7067	130	7.8	-6.2	-5.8
8	0.012	2.8289	150	3.9	-0.56	-0.52
9	0.11	2.9067	178	11	-0.98	-0.90
10	0.060	2.9498	178	75	-0.28	-0.26
11	0.21	2.8111	90	5.9	1.9	1.7
12	0.081	2.8467	90	0.81	3.1	2.9
13	3.0	2.8483	178	10	5.4	4.9
14	0.062	2.8651	178	3.3	1.4	1.2
15	30	2.8651	178	3.3	30	27
16	0.00011	2.9777	178	4.2	0.051	0.046
17	0.0085	2.9776	178	4.2	0.45	0.41
18	0.65	2.9773	90	0.86	-8.7	-7.8
19	81	3.0353	90	0.16	-230	-250
20	0.13	2.9064	178	12	1.0	0.95
21	0.23	2.9497	178	75	0.55	0.50
22	0.00075	3.2372	178	2.0	0.19	0.17
23	0.046	3.2592	178	1.0	-2.1	-1.9
24	0.12	3.2593	178	1.1	-3.3	-2.9
25	0.000082	3.1840	178	0.38	0.15	0.13
26	0.0087	3.1841	178	0.38	-1.5	-1.3
27	0.13	3.1840	178	0.38	5.8	5.1
28	0.00085	3.2379	122	0.099	0.93	0.82
29	0.032	3.2561	122	0.055	7.6	6.7
30	0.090	3.2567	122	0.066	12	10
31	0.13	3.3939	134	0.35	-6.2	-6.7
32	210	3.3948	134	0.069	550	590
33	0.000038	3.0352	90	0.15	-0.16	-0.14
34	2.9	3.4261	178	5.2	-7.5	-6.4
35	0.019	3.4369	90	2.2	0.93	0.79
36	0.000061	3.4293	90	3.2	-0.043	-0.037
37	0.00014	3.4379	90	3.7	-0.061	-0.052
38	0.00012	3.7348	178	0.0012	3.0	2.6
39	0.000014	3.5832	178	2.5	0.023	0.020
40	0.0000070	3.6316	178	0.020	0.19	0.16
41	0.000033	3.9002	90	0.30	0.10	0.085
42	0.0012	3.7349	178	0.0012	10	8.3
43	0.012	3.7668	178	9.1	0.36	0.30
44	0.14	3.8222	130	0.35	-6.4	-5.3
45	0.31	3.8370	178	0.0035	-95	-78
46	0.55	3.8528	178	2.9	-4.4	-3.6

^aThese values correspond to the listed value of β_p .

and for the other nuclei studied are similar.

In Fig. 3 the results are shown as a function of energy (for one resonance pair) for the differential cross section $d\sigma/d\Omega$, the relative enhancement A_z/V , and the figure of merit β_p at a fixed angle $\theta_{\text{c.m.}} = 90^\circ$.

B. Detector segmentation

Although a large solid angle detector would significantly increase the counting rate, the net effect is not immediately obvious, since the angular dependence often includes sign

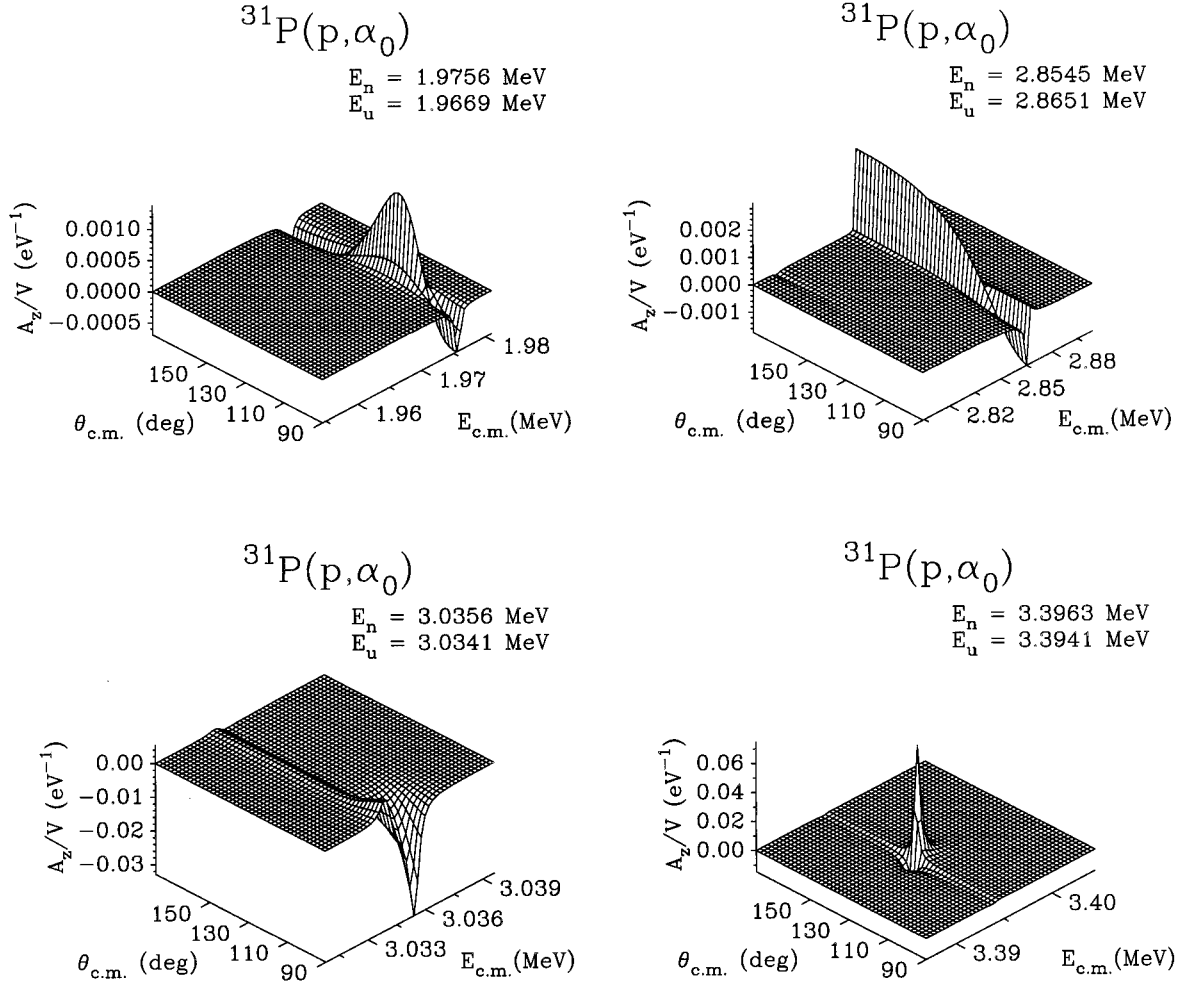


FIG. 1. The enhancement factors A_z/V as functions of energy and angle for four pairs of resonances in $^{31}\text{P}(\vec{p}, \alpha_0)$.

changes in the asymmetry A_z . Our calculations show that in such cases a large solid angle detector may actually reduce the measured A_z . Segmenting the detector is an obvious way to overcome this problem. For a segmented detector with N separate angular regions, the appropriate generalization of the figure of merit is

$$\beta_N = \sum_{i=1}^N \frac{\left\{ \int_{\theta_i}^{\theta_{i+1}} [A_z(\theta)/V] \sigma(\theta) \sin\theta d\theta \right\}^2}{\int_{\theta_i}^{\theta_{i+1}} \sigma(\theta) \sin\theta d\theta}. \quad (14)$$

Our calculations show that a segmented detector is essential, since there are cases where the figure of merit is two orders of magnitude larger for a segmented than for a single detector covering the same angular range. The Legendre polynomials involved in the angular distributions are at most of order 6 or 8, determining the degree of segmentation required to account for these angular effects. (In practice we shall segment to a greater extent in order to minimize counting rates from elastic scattering; see Sec. V.) In Table III the maximum values of the figure of merit β_N are listed as a function of N , the number of segments. Results are listed for $N=1, 4$, and 41 ; the calculations have been performed in angular steps of 2° , and $N=41$ corresponds to a detector

every 2° in the range 90° – 170° . Since there is generally little change in β_N once N reaches 4 or 5, these values of β_{41} are effectively the maximum possible figures of merit that one can obtain by segmenting the detector. Note that there often is a slight change in the energy at which the figure of merit is maximum as N changes.

C. Summary of A_z and β_P ranges

A convenient way to consider the sensitivity of these measurements is to ask how long it would take to measure the parity-violating matrix element V for a given case. Conversely, one can ask what limit is set on V if a null result is obtained after an experiment has been performed for time t . The length of time t can be expressed in terms of the relative enhancement A_z/V , the limit on the matrix element, say, V_L , the number of particles per second in the beam N_b , the number of target nuclei per cm^2 N_t , the differential cross section $d\sigma/d\Omega$, and the total solid angle Ω :

$$t = \left[V_L^2 N_b N_t \Omega \left(\frac{A_z}{V} \right)^2 \frac{d\sigma}{d\Omega} \right]^{-1} \propto \frac{1}{\beta_P V_L^2}. \quad (15)$$

In Fig. 4 the figures of merit are shown for the 46 reso-

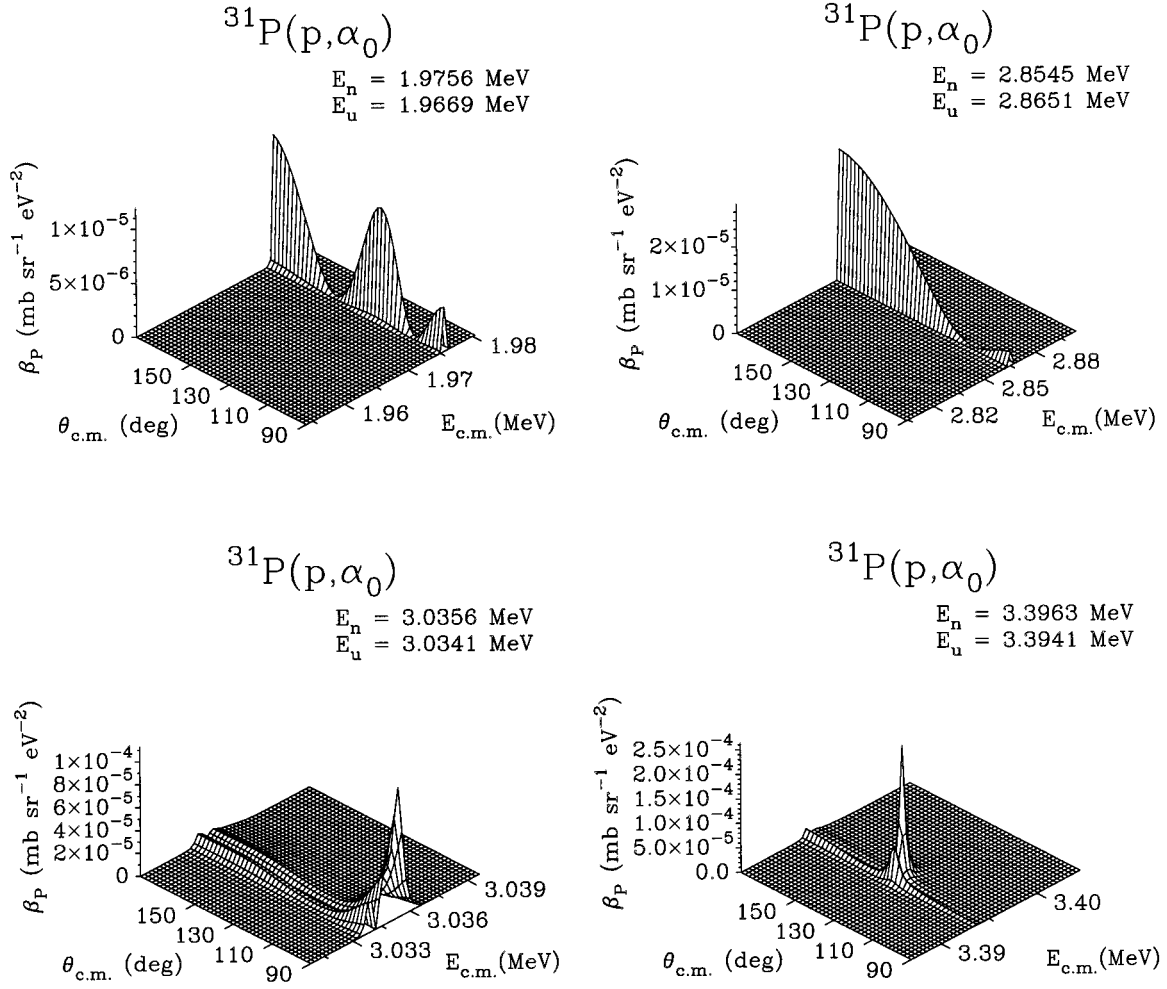


FIG. 2. The figures of merit β_P as functions of energy and angle for the same four pairs of resonances shown in Fig. 1.

nance pairs in the $^{31}\text{P}(\vec{p}, \alpha_0)$ reaction. The values of β_P are shown for a detector segmented into four sections (as shown in Table III, there is generally little change once the degree of segmentation N reaches 4). Note that the figures of merit range over seven orders of magnitude. This emphasizes again the importance of choosing an appropriate resonance for study.

The results for the figures of merit for all five nuclides considered are combined in Fig. 5. From experimental considerations discussed below, we believe that β_P values of order 10^{-6} are needed for realistic experiments. Based on this approximate guideline, the target nuclides ^{31}P and ^{39}K seem most suitable. In previous experiments, the phosphorus target was more stable and uniform, leading to higher quality data. Therefore ^{31}P is our first choice as a target for the study of parity-violation effects in light nuclei.

D. Multilevel effects

In Sec. II we derived the PNC longitudinal asymmetry in the two-level approximation. In general there are several levels that contribute to the parity violation. Since the expressions are very cumbersome in the charged-particle case, we first review the neutron analysis. There the two-level approximation for the PNC longitudinal asymmetry [41–46] is

$$P = 2 \frac{V}{E_s - E_p} \left[\frac{\Gamma_s^n}{\Gamma_p^n} \right]^{1/2}. \quad (16)$$

The expression for the asymmetry P is generalized to include the effects of all of the s -wave resonances on the p -wave resonance in question. If the s -wave resonances are labeled by ν and the p -wave resonances by μ , then

$$P_\mu = 2 \sum_\nu \frac{V_{\mu\nu}}{E_{s\nu} - E_{p\mu}} \left[\frac{\Gamma_{s\nu}^n}{\Gamma_{p\mu}^n} \right]^{1/2} \equiv \sum_\nu A_{\mu\nu} V_{\mu\nu}. \quad (17)$$

If the energies and neutron widths of the s -wave resonances are known, then the A coefficients can be calculated. At first glance this equation appears to make interpretation of the parity-violation results impossible, since there are several unknown values of $V_{\mu\nu}$ for each measured P . It is true that one cannot determine the individual V 's. However, the goal of the experiment is to obtain the rms PNC matrix element, which can be determined.

The PNC matrix elements $V_{\mu\nu}$ are assumed to be Gaussian-distributed random variables with mean zero and variance M^2 :

$$\langle V_{\mu\nu} \rangle = 0, \quad \langle V_{\mu\nu}^2 \rangle = M^2. \quad (18)$$

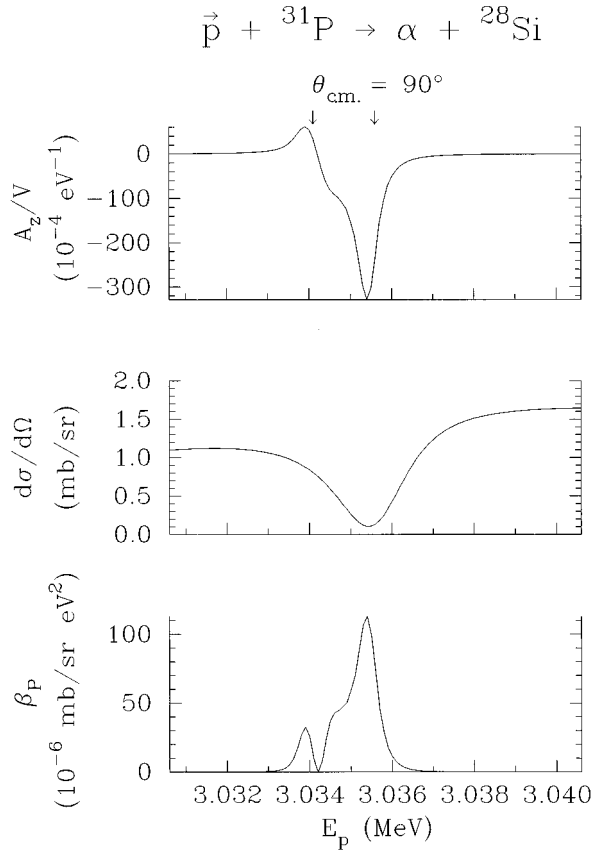


FIG. 3. The quantities A_z/V , $d\sigma/d\Omega$, and β_P as a function of energy at $\theta_{\text{c.m.}}=90^\circ$ for resonance pair No. 19 in ${}^{31}\text{P}(\vec{p}, \alpha_0)$. The behavior of A_z/V and β_P is shown in Figs. 1 and 2. The maximum value of the figure of merit β_P indicates the “best” energy at which to perform the experiment. The vertical arrows indicate the locations of the two resonances.

If the widths and energy spacings are uncorrelated with the matrix elements $V_{\mu\nu}$, then the observables P_μ are also Gaussian-distributed random variables, since the sum of Gaussian random variables is also a Gaussian random variable [47]. Then

$$\langle P_\mu \rangle = 0, \quad \langle P_\mu^2 \rangle = A_\mu^2 M^2, \quad (19)$$

where $A_\mu^2 \equiv \sum_\nu A_{\mu\nu}^2$. Including the experimental uncertainty δ_μ leads to a variance

$$\langle P_\mu^2 \rangle = A_\mu^2 M^2 + \delta_\mu^2. \quad (20)$$

The probability for measuring an asymmetry between P_μ and $P_\mu + dP_\mu$ is

$$\begin{aligned} F(P_\mu) dP_\mu &= \frac{1}{\sqrt{2\pi\langle P_\mu^2 \rangle}} \exp\left[-\frac{P_\mu^2}{2\langle P_\mu^2 \rangle}\right] dP_\mu \\ &= \frac{1}{\sqrt{2\pi(M^2 + \delta_{Q_\mu}^2)}} \exp\left[-\frac{Q_\mu^2}{2(M^2 + \delta_{Q_\mu}^2)}\right] dQ_\mu, \end{aligned} \quad (21)$$

where $Q_\mu \equiv P_\mu/A_\mu$ and $\delta_{Q_\mu} \equiv \delta_\mu/A_\mu$.

These new variables Q_μ also have the property that the mean is zero and the variance is M^2 . This implies that the rms matrix element M can be determined directly from the measured values of P_μ , providing that the $A_{\mu\nu}$ coefficients are known. The details of the analysis procedure are discussed by Bowman *et al.* [48].

Now return to the charged-particle resonance problem. We can proceed in a manner analogous to that followed in the neutron case. However, the equations for A_z are lengthy and cumbersome, since there are generally four to six partial widths and two to four Legendre polynomials in the calculation for each resonance pair. Because of this complexity, we do not include explicit forms of $A_{\mu\nu}$ in the charged-particle case; we simply point out it is still possible to express the asymmetry in the form

$$P_\mu = \sum_\nu A_{\mu\nu} V_{\mu\nu}, \quad (22)$$

and therefore the analysis can proceed in an analogous way to the neutron case, albeit with much more complicated expressions for the $A_{\mu\nu}$ coefficients.

One possible concern about this procedure, for either the neutron or the charged-particle experiment, is that the expression used for the net parity violation is not a true multi-level expression, but instead is a sum of two-level terms: True multilevel effects, such as interference between s -wave resonances in the neutron case, have been ignored. To examine this question, we calculated the asymmetry for three levels (one p -wave and two s -wave resonances or, equivalently, one unnatural-parity and two natural-parity resonances). The general form is the same, but the A coefficients may change. For every neutron example considered, the A coefficients were unchanged from the values obtained from a sum of two-level terms. However, in the three-level charged-particle calculation, the A coefficients did change—the magnitude of the change in A depends on the specific resonance pair, but ranges from a few percent to a maximum of about 30%. The physical origin of this difference can be traced to the size of the average Γ/D . For neutrons the ratio Γ/D is much less than one (of order 10^{-4}), while in the charged-particle case Γ/D is significantly larger (of order 10^{-1}). The details of these considerations will be presented separately [49]. For present purposes we simply note that the ansatz adopted in the neutron analysis also works for charged particles, albeit with some complications.

V. PROPOSED EXPERIMENT

A. Experimental procedure

Measurements of A_z will be made with a longitudinally polarized beam of protons incident on a thin target supported by a thin carbon foil. The alpha particles will be counted in a large solid angle detector at backward angles. Four small surface barrier detectors located at forward angles will detect elastically scattered protons and monitor the product of incident proton flux and target thickness. Measurement of longitudinal asymmetries at the 10^{-4} level requires that the statistical and systematic uncertainties be reduced to the few times 10^{-5} level.

TABLE III. Maximum values of β_N and the corresponding proton energy for $N=1, 4,$ and 41 for resonance pairs in ${}^{31}\text{P}(\vec{p}, \alpha_0)$. The calculations assume a detector covering the range $\theta = 90^\circ - 170^\circ$ and an energy resolution of 500 eV FWHM .

Resonance pair	$N=1$		$N=4$		$N=41$	
	β_1 ($10^{-6} \text{ mb sr}^{-1} \text{ eV}^{-2}$)	E_p (MeV)	β_4 ($10^{-6} \text{ mb sr}^{-1} \text{ eV}^{-2}$)	E_p (MeV)	β_{41} ($10^{-6} \text{ mb sr}^{-1} \text{ eV}^{-2}$)	E_p (MeV)
1	0.031	1.6433	0.031	1.6433	0.031	1.6433
2	0.061	1.9756	3.2	1.9756	3.9	1.9756
3	0.40	1.9890	1.3	1.9890	1.6	1.9890
4	0.010	1.9808	0.010	1.9808	0.010	1.9808
5	0.099	1.9808	0.10	1.9808	0.10	1.9808
6	0.034	2.2574	0.040	2.2574	0.045	2.2574
7	1.5	2.7067	1.5	2.7067	1.5	2.7067
8	0.0081	2.8289	0.0081	2.8289	0.0081	2.8289
9	0.00034	2.9063	0.015	2.9063	0.019	2.9063
10	0.011	2.9494	0.011	2.9498	0.011	2.9498
11	0.12	2.8111	0.12	2.8111	0.12	2.8111
12	0.039	2.8473	0.045	2.8472	0.046	2.8472
13	0.28	2.8489	0.87	2.8481	1.0	2.8480
14	0.028	2.8650	0.028	2.8650	0.028	2.8650
15	4.0	2.8652	6.9	2.8651	7.2	2.8651
16	0.000058	2.9774	0.000059	2.9774	0.000059	2.9774
17	0.0013	2.9778	0.0022	2.9776	0.0023	2.9776
18	0.033	2.9781	0.18	2.9773	0.20	2.9773
19	6.6	3.0339	8.5	3.0339	13	3.0353
20	0.00041	2.9064	0.018	2.9064	0.023	2.9064
21	0.042	2.9497	0.043	2.9497	0.043	2.9497
22	0.00026	3.2372	0.00027	3.2372	0.00027	3.2372
23	0.0015	3.2511	0.0022	3.2511	0.0038	3.2592
24	0.0080	3.2593	0.014	3.2598	0.018	3.2593
25	0.000013	3.1849	0.000019	3.1831	0.000020	3.1831
26	0.0029	3.1838	0.0029	3.1838	0.0029	3.1838
27	0.021	3.1843	0.027	3.1841	0.028	3.1841
28	0.00013	3.2372	0.00021	3.2373	0.00023	3.2375
29	0.00096	3.1968	0.0014	3.1962	0.0032	3.2507
30	0.029	3.2594	0.031	3.2595	0.032	3.2596
31	0.00022	3.3843	0.0079	3.3843	0.013	3.3939
32	7.0	3.3938	8.3	3.3938	16	3.3939
33	0.0000011	3.4259	0.0000037	3.0352	0.0000058	3.0352
34	0.94	3.4258	1.0	3.4258	1.0	3.4258
35	0.0067	3.4386	0.0078	3.4382	0.0079	3.4382
36	0.000025	3.4287	0.000026	3.4287	0.000027	3.4287
37	0.000037	3.4390	0.000053	3.4385	0.000054	3.4385
38	0.0000018	3.5435	0.000020	3.5439	0.000022	3.5439
39	0.0000051	3.5843	0.0000051	3.5843	0.0000051	3.5843
40	0.0000020	3.6412	0.0000021	3.6412	0.0000022	3.6412
41	0.0000092	3.9005	0.000013	3.9002	0.000014	3.9002
42	0.0000056	4.0008	0.000024	3.7327	0.000029	3.7333
43	0.0022	3.7667	0.0022	3.7667	0.0022	3.7667
44	0.044	3.8222	0.056	3.8222	0.061	3.8222
45	0.00027	3.8472	0.034	3.8472	0.041	3.8472
46	0.045	3.8527	0.12	3.8528	0.14	3.8528

The systematic uncertainties are reduced by several means. The azimuthal symmetry of the detector will reduce the sensitivity to many effects, including leading-order contributions from beam misalignment and transverse polariza-

tion components. The proton beam properties will be monitored and controlled to the extent feasible. The proton polarization is varied in a sequence designed to cancel systematic effects. The polarization will be reversed at a 10 Hz

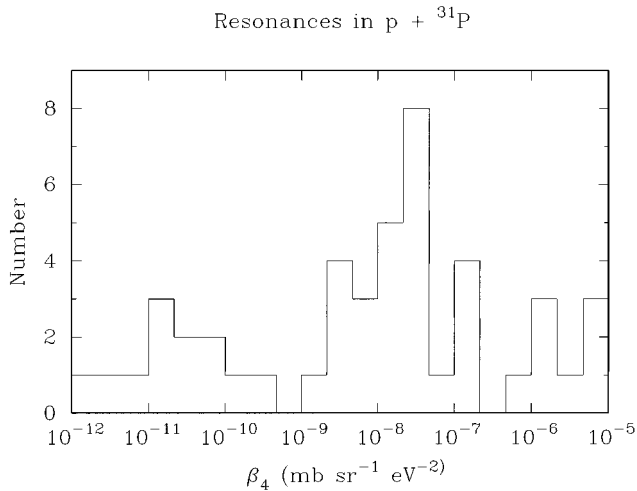


FIG. 4. The maximum figures of merit β_p (for a detector segmented into four ranges of θ) for resonance pairs in $^{31}\text{P}(p, \alpha_0)$.

rate in an eight-step sequence $+ - - + - + + -$, which cancels detector drifts to second order [50]. The proton energy will be ramped over the resonance of interest with a period of approximately 100 s in energy steps of about 50 eV, which allows subtraction of the background (off-resonance) asymmetry from the PNC (on-resonance) asymmetry.

Special efforts will be made to monitor and/or control the proton beam properties, including position on target, energy, polarization, and intensity. Horizontal and vertical components of beam position will be monitored. A special feedback system will take current readings following the analyzing magnet system and generate a signal to the carbon stripper foil in the terminal of the tandem. Preliminary tests indicate [51] that this reduces the terminal fluctuations to less than 100 eV, and also improves position stability. The average transverse polarization moments will be monitored by the four detectors located at forward angles. Higher-order polarization moments arising from inhomogeneous polarization distributions [52] also will be determined.

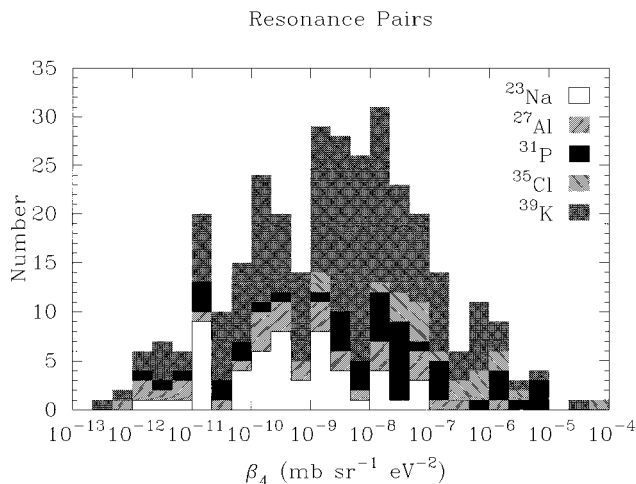


FIG. 5. The maximum figures of merit β_p (for a detector segmented into four ranges of θ) for resonance pairs in five $2s-1d$ shell nuclei.

The alpha particle detector must subtend a large solid angle (approaching 2π), be segmented in θ , and have sufficient energy resolution to separate the alpha particles from the elastically scattered protons. The (p, α) reactions employed are exoergic and the resulting spectra are rather simple. However, the proton-counting rates are so high that the counting rate considerations require a higher degree of segmentation than do the effects of the angular dependence of the parity violation. A silicon strip detector seems ideal for these measurements. The tentative design involves commercially available silicon strip detectors that are trapezoidal in shape and segmented into 16 strips per detector. Each detector would cover an octant with the four detectors arranged in the shape of a pyramid, covering the angular range $100^\circ \leq \theta \leq 170^\circ$ and $0^\circ \leq \phi \leq 360^\circ$. There will be 64 channels of electronics. This approach is similar to that described by Wuosmaa *et al.* [53]. Because of the positive Q value for the reaction, typically 2 MeV, analog-to-digital converter (ADC) gates can be generated only for the alpha particles. Because of the unique geometry and of the concerns about position stability, etc., a dedicated chamber will be designed and constructed for this experiment.

B. Numerical estimates

Equation (15) can be used to estimate the time required to reach a given limit on V , $t = (k\beta_p V^2)^{-1}$. The constant k reflects the experimental conditions: the beam intensity, the target thickness, and the detector solid angle. A reasonable estimate of the maximum polarized beam is about 500 nA, the target thickness is of order $10 \mu\text{g}/\text{cm}^2$, and the maximum solid angle is 2π . If we adopt $10^{-6} \text{ mb}/(\text{sr eV}^2)$ as a convenient standard unit for β_p and have V in eV, then the expression reduces to $t \approx 133/\beta_p V^2$, with t in seconds. Then for $\beta_p = 1$ (in units of 10^{-6}), a limit of $V = 50 \text{ meV}$ corresponds to $5 \times 10^4 \text{ s}$ or about 0.5 day. For a typical average spacing of $D = 50 \text{ keV}$, a determination of $V = 50 \text{ meV}$ would correspond to a weak spreading width of a few times 10^{-7} , comparable to the value observed in heavy nuclei by the neutron PNC measurements.

Another approach is to assume that no parity violations are observed. For ^{31}P there are eight resonance pairs with values of $\beta_p \geq 1 \times 10^{-6}$. For these resonances the limits on V placed by a null result after 1 day of measurement would be 20 meV (resonance pair No. 2), 31 meV (No. 3), 32 meV (No. 7), 39 meV (No. 13), 15 meV (No. 15), 11 meV (No. 19), 10 meV (No. 32), and 39 meV (No. 34). This would correspond to an average limit of about 25 meV on the rms matrix element, and would imply that the weak spreading width is significantly smaller in light nuclei than in heavy nuclei. Therefore even this set of null results would be quite important.

VI. SUMMARY

The recent measurements of parity violation in neutron resonances in heavy nuclei suggest that the determination of PNC matrix elements in light nuclei be given a high priority. We have considered parity violation in the (p, α) reaction using experimental resonance parameters for five $2s-1d$ nuclei. We obtained predictions for 331 resonance pairs for the

relative enhancement of the longitudinal analyzing power. This ratio shows striking sensitivity to energy, angle, and the specific resonance pair. A figure of merit involving both the relative enhancement and the differential cross section was calculated for each resonance pair. Assuming that the weak spreading width has the value obtained in the neutron measurements on heavy nuclei, an estimate for the local V_{rms} was obtained for each resonance pair. This provides an estimate for each of the 331 resonance pairs. Numerical results are given for the ^{31}P resonance pairs. The proposed experimental procedure was described. Particular emphasis was placed on the design of a segmented detector. Examples using reasonable values for experimental parameters indicate that

charged-particle resonance studies of parity violation are quite feasible.

ACKNOWLEDGMENTS

This work was supported in part by the U.S. Department of Energy, Office of High Energy and Nuclear Physics, under Grants Nos. DE-FG05-87-ER40353 and DE-FG05-88-ER40441. The authors would like to thank D. P. Balamuth, H. L. Harney, N. R. Roberson, H. A. Weidenmüller, and W. S. Wilburn for informative discussions. We especially wish to thank W. S. Wilburn for suggesting the proposed design of the charged-particle detector.

-
- [1] V. P. Alfimenkov, S. B. Borzakov, Vo Van Thuan, Yu. D. Mareev, L. B. Pikelner, A. S. Khrykin, and E. I. Sharapov, *Nucl. Phys.* **A398**, 93 (1983).
- [2] O. Bohigas and H. A. Weidenmüller, *Annu. Rev. Nucl. Part. Sci.* **38**, 421 (1988).
- [3] J. D. Bowman, G. T. Garvey, Mikkel B. Johnson, and G. E. Mitchell, *Annu. Rev. Nucl. Part. Sci.* **43**, 829 (1993).
- [4] E. G. Adelberger and W. C. Haxton, *Annu. Rev. Nucl. Part. Sci.* **35**, 501 (1988).
- [5] P. A. Krupchitsky, *Fundamental Research with Polarized Slow Neutrons* (Springer-Verlag, Berlin, 1987).
- [6] O. P. Sushkov and V. V. Flambaum, *JETP Lett.* **32**, 352 (1980).
- [7] O. P. Sushkov and V. V. Flambaum, *Sov. Phys. Usp.* **25**, 1 (1982).
- [8] S. A. Biryukov *et al.*, *Sov. J. Nucl. Phys.* **45**, 937 (1987).
- [9] Y. Masuda, T. Adachi, A. Masaike, and K. Morimoto, *Nucl. Phys.* **A504**, 269 (1989).
- [10] V. W. Yuan *et al.*, *Phys. Rev. C* **44**, 2187 (1991).
- [11] H. Benkoula, J. C. Cavaignac, J. L. Charvet, D. H. Koang, B. Vignon, and R. Wilson, *Phys. Lett.* **71B**, 287 (1977).
- [12] M. Forte, B. R. Heckel, N. F. Ramsey, K. Green, G. L. Greene, J. Byrne, and J. M. Pendlebury, *Phys. Rev. Lett.* **45**, 2088 (1980).
- [13] B. Heckel *et al.*, *Phys. Lett.* **119B**, 298 (1982).
- [14] V. A. Vesna, É. A. Kolomenskiĭ, V. M. Lobashev, V. A. Nazarenko, A. N. Pirozhkov, L. M. Smotriskiĭ, Yu. V. Sobolev, and N. A. Titov, *JETP Lett.* **36**, 209 (1982).
- [15] X. Zhu *et al.*, *Phys. Rev. C* **46**, 768 (1992).
- [16] C. M. Frankle *et al.*, *Phys. Rev. C* **46**, 778 (1992).
- [17] Y.-F. Yen *et al.*, in *Polarization Phenomena in Nuclear Physics*, edited by E. J. Stephenson and S. E. Vigdor, AIP Conf. Proc. No. 339 (AIP, New York, 1995), p. 136.
- [18] J. F. Shriner, Jr. and G. E. Mitchell, *Phys. Rev. C* **49**, R616 (1994).
- [19] J. R. Vanhoy, E. G. Bilpuch, C. R. Westerfeldt, and G. E. Mitchell, *Phys. Rev. C* **36**, 920 (1987).
- [20] R. O. Nelson, E. G. Bilpuch, C. R. Westerfeldt, and G. E. Mitchell, *Phys. Rev. C* **29**, 1656 (1984); **30**, 755 (1984).
- [21] C. T. Coburn, J. F. Shriner, Jr., and C. R. Westerfeldt, *Z. Phys.* **A 343**, 185 (1992).
- [22] D. F. Fang, E. G. Bilpuch, C. R. Westerfeldt, and G. E. Mitchell, *Phys. Rev. C* **37**, 28 (1988).
- [23] W. K. Brooks, Ph.D. thesis, Duke University, 1988.
- [24] B. J. Warthen, Ph.D. thesis, Duke University, 1987.
- [25] J. S. Bull, Ph.D. thesis, Duke University, 1989.
- [26] J. F. Shriner, Jr., E. G. Bilpuch, P. M. Endt, and G. E. Mitchell, *Z. Phys. A* **335**, 393 (1990).
- [27] J. F. Shriner, Jr., G. E. Mitchell, and T. von Egidy, *Z. Phys. A* **338**, 309 (1991).
- [28] W. E. Ormand and R. A. Broglia, *Phys. Rev. C* **46**, 1710 (1982).
- [29] V. Zelevinsky, M. Horoi, and B. A. Brown, *Phys. Lett. B* **350**, 141 (1995).
- [30] R. O. Nelson, E. G. Bilpuch, and G. E. Mitchell, *Nucl. Instrum. Methods Phys. Res. A* **236**, 128 (1985).
- [31] A. M. Lane and R. G. Thomas, *Rev. Mod. Phys.* **30**, 257 (1958).
- [32] A. Simon, *Phys. Rev.* **92**, 1050 (1953).
- [33] G. R. Satchler, *Proc. Phys. Soc. London A* **68**, 1041 (1955).
- [34] P. Heiss, *Z. Phys.* **251**, 159 (1972).
- [35] D. M. Brink and G. R. Satchler, *Angular Momentum*, 2nd ed. (Oxford University Press, Oxford, 1968).
- [36] L. C. Biedenharn, J. M. Blatt, and M. E. Rose, *Rev. Mod. Phys.* **24**, 249 (1952).
- [37] R. Huby, *Proc. Phys. Soc. London A* **67**, 1103 (1954).
- [38] H. L. Harney, A. Richter, and H. A. Weidenmüller, *Rev. Mod. Phys.* **58**, 607 (1986).
- [39] G. E. Mitchell, C. R. Bybee, J. M. Drake, E. G. Bilpuch, and J. F. Shriner, Jr., in *Time Reversal Invariance and Parity Violation in Neutron Reactions*, edited by C. R. Gould, J. D. Bowman, and Yu. P. Popov (World Scientific, Singapore, 1994), p. 167.
- [40] J. M. Drake, E. G. Bilpuch, G. E. Mitchell, and J. F. Shriner, Jr., *Phys. Rev. C* **49**, 411 (1994).
- [41] V. E. Bunakov and V. P. Gudkov, *Z. Phys. A* **303**, 285 (1981).
- [42] V. P. Alfimenkov, *Sov. Phys. Usp.* **27**, 11 (1984).
- [43] J. R. Vanhoy, E. G. Bilpuch, J. F. Shriner, Jr., and G. E. Mitchell, *Z. Phys. A* **331**, 1 (1988).
- [44] C. R. Gould, D. G. Haase, N. R. Roberson, H. Postma, and J. D. Bowman, *Int. J. Mod. Phys. A* **5**, 2181 (1990).
- [45] V. E. Bunakov and V. P. Gudkov, *Nucl. Phys.* **A401**, 93 (1983).
- [46] B. Desplanques, *J. Phys. (Paris) Colloq.* C3-2 **45**, 55 (1984).
- [47] W. T. Eadie, D. Drijard, F. E. James, M. Roos, and B. Sadou-

- let, *Statistical Methods in Experimental Physics* (North-Holland, Amsterdam, 1971).
- [48] J. D. Bowman, L. Y. Lowie, G. E. Mitchell, E. I. Sharapov, and Yi-Fen Yen, *Phys. Rev. C* **53**, 285 (1996).
- [49] J. F. Shriner, Jr. and G. E. Mitchell (unpublished).
- [50] N. R. Roberson *et al.*, *Nucl. Instrum. Methods Phys. Res. A* **326**, 549 (1993).
- [51] W. S. Wilburn, N. R. Roberson, and C. Y. Scarlett, *Bull. Am. Phys. Soc.* **40**, 1619 (1995).
- [52] M. Simonius, R. Henneck, Ch. Jacquemart, and J. Lang, *Nucl. Instrum. Methods* **177**, 471 (1980).
- [53] A. H. Wuosmaa *et al.*, *Nucl. Instrum. Methods Phys. Res. A* **345**, 482 (1994).